Thermo-elastic analysis of rotating functionally graded micro-discs incorporating surface and nonlocal effects

Farzad Ebrahimi*[1] and Ebrahim Heidari

Department of Mechanical Engineering, Faculty of Engineering, Imam Khomeini International University, Qazvin, Iran

Abstract. This research studies thermo-elastic behavior of rotating micro discs that are employed in various micro devices such as micro gas turbines. It is assumed that material is functionally graded with a variable profile thickness, density, shear modulus and thermal expansion in terms of radius of micro disc and as a power law function. Boundary condition is considered fixed-free with uniform thermal loading and elastic field is symmetric. Using incompressible material's constitutive equation, we extract governing differential equation of four orders; to solution this equation, we utilize general differential quadrature (GDQ) method and the results are schematically pictured. The obtained result in a particular case is compared with another work and coincidence of results is shown. We will find out that surface effect tends to split micro disc's area to compressive and tensile while nonlocal parameter tries to converge different behaviors with each other; this convergence feature make FGIMs capable to resist in high temperature and so in terms of thermo-elastic behavior we can suggest, using FGIMs in micro devices such as micro turbines (under glass transition temperature).

1. Introduction

Functionally graded materials are originally a category of composite materials in which the distribution of components gradually change in one or multiple directions to obtain tailored material property; for example, Chakraborty *et al.* (2009), explained how a graded composite of silver and alumina can simultaneously combine hardness (emanated from alumina) and toughness (emanated from silver), which can be efficient to use for cutting tools. Reports of this sort that are based on combination of metals and ceramics are numerous (Agari 2002). The other types of functionally graded materials are rubber like FGMs, which are made from different types of polymers. Polyvinyl chloride (PVC)/polymethacrylate, polymethyl methacrylate (PMMA), polyhexyl methacrylate (PHMA), bisphenol A type polycarbonate (PC)/polystyrene (PS), PEO/polybutyl methacrylate (PBMA) are some of examples of rubber like FGMs (Agari *et al.* 1996). Presenting novel properties, FGMs have also attracted intensive research interests, which were mainly focused on their static, dynamic and vibration characteristics of FG structures (Ebrahimi and Rastgoo 2008a, b, c, Ebrahimi 2013, Ebrahimi *et al.* 2008, 2009a, b, 2016a,

---

∗Corresponding author, Professor, E-mail: febrahimy@eng.ikiu.ac.ir

Ebrahimi and Zia 2015, Ebrahimi and Mokhtari 2015, Ebrahimi *et al*. 2015, Ebrahimi and Salari 2015, Ebrahimi and Jafari 2016, Ebrahimi and Barati 2017a, b, Ebrahimi and Barati *et al*. 2017, Ebrahimi and Ehyaei *et al*. 2017). Among different ways to produce such materials, Agari *et al*. (1996), have devised a new method that is called dissolution-diffusion method that is performed in a very fewer time with optimized conditions such as low temperature; In this method since there is minimum of interface during compositional gradient we will obtained higher strength and more thermal shock resistance (Agari *et al*. 2007). Anyway, if there are a lot of manufacturing errors, it will result in a sharp decline in the quality; Carmine and Quadrini (2009), have tried to diminish such errors by using indented instruments. The other factor that is able to decline the quality and mechanical property of rubber like materials is inhomogeneity. Rajagopal (1994), in his research, makes evident that temperature gradient can develop boundary layer-like structures in strain field of rubber like material and finally, inhomogeneity will be obtained. However, Bilgili (2004) explained that functional grading of this material makes inhomogeneity to be decreased even in the presence of temperature gradient. He also said that functional grading of rubber like materials helps them to control their mechanical response in thermally antagonistic environments; But there is one exception, when rubber like materials are vulcanized; in this situation even functional grading is not able to prevent from developing localized and complex stress-deformation fields and inhomogeneity is inevitable specially in shear modulus. It is for that, when to curing, the core is subjected to heat less than the surface of material (Bilgili 2003).

Rubber like materials are considered as incompressible materials because their Poisson's ratio is around 0.5; although the ratio of the bulk to shear modulus (B/G) is determinant factor of being compressible or incompressible, the bulk modulus (B) of rubber like materials is not too large; as more explanation, when Poisson's ratio approaches 0.5 the ratio of bulk to shear approaches to infinite which could be for two reason: First, having large bulk; second, as G is too smaller than bulk modulus which is common in rubber like materials. Although water is not a rubber like material but it could be a good example to understand what happens about rubber like materials; as more explanation, water cannot undergo shear force and therefore the shear modulus of water is zero, however it is known as an incompressible material (Mott *et al*. 2008).

As an important component, discs have many engineering applications; turbo generators, turbojet engines and turbine rotors are some of examples of the applications of discs; this is the reasons for attracting many researchers to investigate about rotating discs; for example, Zenkour (2006) studied various functionally graded annular discs with variable thickness under steady heat flow condition. Horgan and Chan (1999), with the purpose of studying of inhomogeneity effect, investigated the stress response of functionally graded rotating discs with power law variation in module of elasticity, and found out different behavior than homogeny cases such as different position of maximum stresses and so forth. Jahed *et al*. (2005), used varied thickness and material properties to achieve optimum mass for the rotating disc in high temperature situation like what takes place in gas turbines. Eraslan and Akis (2006), performed an analytical plane strain and plane stress solutions on the functionally graded rotating solid shaft and solid disc with assumption of exponential and parabolic variation for modulus of elasticity, and found out independency between stresses and the variation of the modulus of elasticity; they also discovered that hoop and radial stresses are equal. Kordkheili and Nghdabadi (2007), performed a comparative study between semi-analytical and finite element solution on functionally graded rotating disc and then studied the role of property gradation on thermomechanical responses. Using Airy stress function Nie and Batra (2010), analyzed stresses in isotropic functionally graded incompressible rotating discs with variable thickness, shear modulus, thermal expansion coefficient and density; they

finally tailored variation of shear modulus and thermal coefficient expansion to reach constant combination of hoop and radial stresses. Dryden and Batra (2013) performed finite plane strain analyzing for hollow cylinders made of Mooney-Rivlin material with the purpose of material tailoring under tangential traction and displacement constrain on the inner and outer surface; they supposed varying material moduli in radial direction and concluded that radial variation of moduli minimizes the tangential displacement when tangential traction is specified. Hosseini and Dini (2015) provided an analytical solution of elasticity's special parameters (displacement, strain and stress) for a rotating thick-walled cylinder made of functionally graded material under thermal and magnetic effects. Tutuncu and Temel (2013), used complementary functions method (CFM) to analyze the thermo-elastic problem of functionally graded rotating discs of variable thickness and uniform change in temperature. Ding *et al*. (2014), with analytical solution, evaluated thermal loading in order to material tailoring in rotating disc. Zamani *et al*. (2014), simulated numerically an annular rotating disc in high speed state and did a comparison with analytical result. Çetin *et al*. (2014), made elastic stress analysis for annular bi-material rotating disc under mechanical and thermomechanical loads; by applying thickness variation they found out that thickness of profiles play an important role in determining stress responses. Ersalan and Ahmet (2015) accomplished an analytical and numerical solution to a rotating FGM Disc by assigning a new exponential model for the modulus of elasticity. Leu and Chien (2015) performed a thermoelastic analysis for a functionally graded disc with non-uniform heat source and on the assumption that thickness changes as a power function of radius. Zafarmand and Kadkhodayan (2015) accomplished their research on functionally graded nanocomposite rotating disc assuming that relations are nonlinear and the thickness is variable; they discovered that in high angular velocities the difference between linear and nonlinear results are noticeable. Anani *et al*. (2016), carried out their stress analysis over rotating thick wall shell that was made from functionally graded incompressible hyperelastic material; they concluded that inhomogeneity has significant influence on mechanical behavior of the cylinder.

In the small scale, rotating micro disc is one of prominent elements can be used in micro gas turbines (MGTs). Compared with the conventional gas turbine, the micro gas turbine has the advantages of small size, light weight, and high power density energy. The application prospect is very broad in the future (Zhen *et al*. 2015); meanwhile reports have been put out based on decreasing electricity costs between 10% and 40% and decreasing of greenhouse gases by 20%-35% (Aichmayer *et al*. 2013), so they can be very efficient and appropriate for environment; the internal temperature in such devices can reach up to 950°C (Zhou *et al*. 2014). However, in the small scale the classical elasticity theories are not applicable; the nonlocal elasticity theory is one of the common approaches which are used to study the behavior of structures in the small scale; Lots of studies have been performed to investigate the scale-dependent response of structural systems based on Eringen's nonlocal elasticity theory (Ebrahimi and Salari 2015a, b, 2016, Ebrahimi *et al*. 2015a, 2016c, Ebrahimi and Nasirzadeh 2015, Ebrahimi and Barati 2016 a-f, Ebrahimi and Hosseini 2016 a-c). Again, based on Eringen's nonlocal elasticity theory Zhu and Li (2017) studied the twisting static behaviors of functionally graded nanotubes. The other theory which can be useful in studying small scale structures is surface elasticity theory. Using surface and nonlocal elasticity theory Ebrahimi *et al*. (2016) investigated vibration and buckling behavior of nanotubes in thermal environment considering different boundary conditions. Most recently Ebrahimi and Barati (2016g, h, i, j, k, l, m, n, o, p, q, r, s, t, u, v, 2017a, b) and Ebrahimi *et al*. (2017) explored thermal and hygro-thermal effects on nonlocal behavior of FG nanobeams and nanoplates.
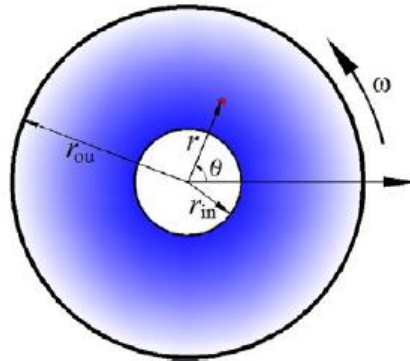
Fig.1 Schematic sketch of the case study

One of the main elements of MGTs is impeller which can be modeled as a rotating micro-disc. Since functionally graded incompressible materials (FGIMs), can potentially control their mechanical response in thermally destructive environment, this scrip tries to study different effects on FGIMs micro rotating discs aiming to use them in micro devices such as MGTs; to do this, we use Eringen's nonlocal elasticity theory in conjunction with surface elasticity theory to derive governing equations for rotating circular micro-disc made of incompressible functionally graded material under fixed-free boundary condition (the boundary condition at inner radius is fixed while at outer radius we have free boundary condition) in thermal environment; it is assumed that the angular velocity is constant and shear modulus, the mass density, the thermal expansion coefficient and the disc thickness alternate as power-law function; assuming linear strain-displacement relations, uniform temperature rise and existence of constant pressure on the free radius, we use GDQ method to study the effect of different parameters on stress, strain and displacement developed in the micro-disc.

2. Formulation of problem

Assume a symmetric rotating circular micro-disc of incompressible functionally graded material (FGIM) with a variable thickness h(r)>0 in the radial direction, and with a constant angular velocity, ω, about the perpendicular axis passing through the center of disc, as shown in Fig. 1 Neglecting gravitational forces, the equation of equilibrium in the radial direction is (Timoshenko and Goodier 1970).

$$\frac{d}{dr}(h(r)r\sigma_r^{nl}) - h(r)\sigma_\theta^{nl} + h(r)\rho(r)\omega^2 r^2 = 0 \qquad (1)$$

Where σ_r^{nl}, and σ_θ^{nl} are nonlocal radial and hoop stresses respectively; $\rho(r)$ is the variable mass density that changes in terms of r. According to nonlocal theory the stress at a reference point r in the body depends not only on the strains at x but also on strains at all other points of the body; in the small scales like micro and nano this dependency becomes more evident as deduced from the following equation (Eringen 2002).

$$\sigma_{ij}^{nl} = \int_v \alpha(|r' - r|, \tau)\sigma_{ij}^{cl}(r')dv(r') \qquad (2)$$

where v is whole volume of a body, τ is a material constant, σ^{cl} is a Cauchy's stress with respect to classical elasticity theory and $\alpha(|r' - r|, \tau)$ is the nonlocal modulus with a dependency of scale factor $|r' - r|$. $\alpha(|r' - r|, \tau)$ is a Green's function and its operator is (Eringen 2002).

$$L: 1 - \mu_{ss}\nabla^2 = 1 - \mu_{ss}\left(\frac{\partial^2}{\partial r^2} + \frac{1}{r}\frac{\partial}{\partial r} + \frac{\partial^2}{r^2 \partial \theta^2}\right) \tag{3}$$

Using this operator, Eq. (4) is used instead of complicated Eq. (2).

$$(1 - \mu_{ss}\nabla^2)\sigma^{nl} = \sigma^{cl} \tag{4}$$

From cinematic relations we have

$$\varepsilon_r = \frac{du_r}{dr}, \qquad \varepsilon_\theta = \frac{u_r}{r} \tag{5a, 5b}$$

And the compatibility equation in terms of strains is

$$\frac{d}{dr}(r\varepsilon_\theta) - \varepsilon_r = 0 \tag{6}$$

The strains can be divided in two parts, elastic and thermal

$$\varepsilon_r = \varepsilon_r^e + \varepsilon_r^T \tag{7a}$$

$$\varepsilon_\theta = \varepsilon_\theta^e + \varepsilon_\theta^T \tag{7b}$$

$$\varepsilon_z = \varepsilon_z^e + \varepsilon_z^T \tag{7c}$$

where

$$\varepsilon_r^T = \varepsilon_\theta^T = \varepsilon_z^T = \alpha(r)\Delta T \tag{8}$$

According to definition of incompressible materials

$$\varepsilon_r^e + \varepsilon_\theta^e + \varepsilon_z^e = 0 \tag{9}$$

For the incompressible material Poisson's ratio is equal to 0.5 ($\upsilon=0.5$) and special constitutive equation shall be used for them

$$\sigma_{ij}^{cl} = -p(r) + 2G(r)\varepsilon_{ij} \tag{10}$$

where p(r) is an arbitrary function which shall be determined from boundary conditions and G(r) is the variable shear modulus.

For this constitutive equation we should introduce appropriate surface effect; According Gurtin and Murdoch theory for the second Piola Kirchhoff surface stress tensor we can write (Gurtin and Murdoch 1975).

$$\hat{S} = I\sigma + ICE + \nabla u \, \sigma \tag{11}$$

where C is elasticity tensor, E is the infinitesimal strain, σ is the residual stress, u is displacement and $\hat{S}$ is second Piola Kirchhoff surface stress tensor. According constitutive equation Eq. (10) we have

$$CE = qI + 2\mu^s E \tag{12}$$

From Eq. (11) and Eq. (12)

$$\hat{S} = I\sigma + qI + 2\mu^s IE + \nabla u\,\sigma \tag{13}$$

And for Cauchy's stress

$$S = \sigma I + 2(\mu^s - \sigma) + qI + \sigma\,\nabla_s u \tag{14}$$

Knowing that $q = -p(r)$ the Eq. (14) gives

$$S_{\alpha\beta} = \sigma\delta_{\alpha\beta} + 2(\mu^s - \sigma)\varepsilon_{\alpha\beta} - p(r)\delta_{\alpha\beta} + \sigma\frac{\partial u_\alpha^s}{\partial x_\beta}, \qquad \alpha, \beta = r, \theta \tag{15a}$$

$$S_{\alpha z} = \sigma\frac{\partial u_z^s}{\partial x_\alpha} \tag{15b}$$

Since the body forces are in the radial direction, we can conclude the affection of the surface will be in this direction. According to Gurtin and Murdoch theory the surface equilibrium equation is (Gurtin and Murdoch 1975).

$$div\,S - Tn = \rho_0\ddot{u} \quad \text{on the boundary surface} \tag{16}$$

In the radial direction, on the lateral surface of disc this equation turns into

$$\frac{\partial S_{\theta r}}{\partial r} + \frac{\partial S_{\theta z}}{\partial z} - \sigma_r = \rho\ddot{u}_r \tag{17}$$

where σ_r is Cauchy's stress. Now we are able to introduce surface effect into constitutive equations by following function (Lu *et al*. 2006)

$$\sigma'_r = \frac{r}{R}\left[\frac{\partial S_{\theta r}}{\partial r} + \frac{\partial S_{\theta z}}{\partial z} - \rho\ddot{u}_r\right]_{r=R} \tag{18}$$

By above consideration the constitutive equations turn into

$$\sigma_r^{cl} = -p(r) + 2G(r)\varepsilon_r^e + \frac{r}{R}\left[\frac{\partial S_{\theta r}}{\partial r} + \frac{\partial S_{\theta z}}{\partial z} - \rho\ddot{u}_r\right]_{r=R} \tag{19a}$$

$$\sigma_\theta^{cl} = -p(r) + 2G(r)\varepsilon_\theta^e \tag{19b}$$

$$\sigma_z^{cl} = -p(r) + 2G(r)\varepsilon_z^e \tag{19c}$$

where according to Eq. (15)

$$S_{\theta r} = 2(\mu^s - \sigma)\varepsilon_{r\theta} \tag{20a}$$

$$S_{\theta z} = 2(\mu^s - \sigma)\varepsilon_{\theta z} + \sigma\frac{\partial u_\theta^s}{\partial z} \tag{20b}$$

$$\rho\ddot{u}_r = \rho r\omega^2 \tag{20c}$$

From (19) and (20) we have

$$\sigma_r^{cl} = -p(r) + 2G(r)\varepsilon_r^e + \frac{r}{R}\left[2(\mu^s - \sigma)\varepsilon_{r\theta,r} + 2(\mu^s - \sigma)\varepsilon_{\theta z,z} + \sigma u_{\theta,zz}^s - \rho^s r\omega^2\right]_{r=R} \tag{21a}$$

$$\sigma_\theta^{cl} = -p(r) + 2G(r)\varepsilon_\theta^e \tag{21b}$$

$$\sigma_z^{cl} = -p(r) + 2G(r)\varepsilon_z^e \tag{21c}$$

The symmetry assumption gives

$$u_\theta = 0, \qquad \frac{\partial}{\partial \theta} = 0 \tag{22}$$

From Eq. (22) we can conclude that

$$\varepsilon_{r\theta} = 0, \qquad \varepsilon_{\theta z} = 0 \tag{23}$$

So, Eq. (21) becomes

$$\sigma_r^{cl} = -p(r) + 2G(r)\varepsilon_r^e - \rho^s r \omega^2 \tag{24a}$$

$$\sigma_\theta^{cl} = -p(r) + 2G(r)\varepsilon_\theta^e \tag{24b}$$

$$\sigma_z^{cl} = -p(r) + 2G(r)\varepsilon_z^e \tag{24c}$$

For nonlocal stresses we use Eq. (4)

$$(1 - \mu_{ss}\nabla^2)\sigma_r^{nl} = \sigma_r^{cl} = -p(r) + 2G(r)\varepsilon_r^e - \rho^s r \omega^2 \tag{25a}$$

$$(1 - \mu_{ss}\nabla^2)\sigma_\theta^{nl} = \sigma_\theta^{cl} = -p(r) + 2G(r)\varepsilon_\theta^e \tag{25b}$$

$$(1 - \mu_{ss}\nabla^2)\sigma_z^{nl} = \sigma_z^{cl} = -p(r) + 2G(r)\varepsilon_z^e \tag{25c}$$

Since $\sigma_z^{nl} = 0$ from Eq. (25c) we can conclude

$$\varepsilon_z^e = \frac{-p(r)}{2G(r)} \tag{26}$$

From Eqs. (26) and (9) we have

$$p(r) = -2G(r)(\varepsilon_r^e + \varepsilon_\theta^e) \tag{27}$$

Using Eqs. (25a), (25b) and (27) we have

$$\varepsilon_r^e = \frac{2\bar{A} - \bar{B}}{6G(r)}, \qquad \varepsilon_\theta^e = \frac{2\bar{B} - \bar{A}}{6G(r)} \tag{28a, 28b}$$

$$\bar{A} = (1 - \mu_{ss}\nabla^2)\sigma_r^{nl} + \rho^s r \omega^2, \qquad \bar{B} = (1 - \mu_{ss}\nabla^2)\sigma_\theta^{nl} \tag{28c}$$

From Eqs. (7), (8) and (28) we can write

$$\varepsilon_r = \varepsilon_r^e + \varepsilon_r^T = \frac{2\bar{A} - \bar{B}}{6G(r)} + \alpha(r)\Delta T \tag{29a}$$

$$\varepsilon_\theta = \varepsilon_\theta^e + \varepsilon_\theta^T = \frac{2\bar{B} - \bar{A}}{6G(r)} + \alpha(r)\Delta T \tag{29b}$$

3. Solution procedure

In terms of the Airy stress function $\varphi(r)$, stresses σ_r^{nl} and σ_θ^{nl} are given by
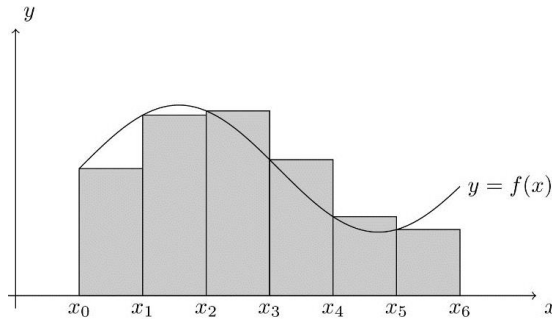
Fig. 2 Schematic for Riemann summation

$$\sigma_r^{nl} = \frac{\varphi(r)}{h(r)r} \ , \qquad \sigma_\theta^{nl} = \frac{1}{h(r)}\frac{d\varphi(r)}{dr} + \rho(r)\omega^2 r^2 \qquad \text{(30a, 30b)}$$

Using Eqs. (29), (30) into compatibility Eq. (6) we get

$$f_4 \frac{\partial^4 \varphi}{\partial r^4} + f_3 \frac{\partial^3 \varphi}{\partial r^3} + f_2 \frac{\partial^2 \varphi}{\partial r^2} + f_1 \frac{\partial \varphi}{\partial r} + f_0 \varphi + f = 0 \qquad (31)$$

where,

$$f_4 = -\frac{1}{3}\frac{r\mu_{ss}}{G(r)h(r)} \qquad (32a)$$

$$f_3 = \frac{6Gh^2 h' \mu_{ss} r^3 + 2G' h^3 \mu_{ss} r^3 - 4Gh^3 \mu_{ss} r^2}{6r^2 h(r)^4 G(r)^2} \qquad (32b)$$

$$f_2 = \frac{-4hh'G'r\mu_{ss} + 6hh''Gr\mu_{ss} - 12h'^2 Gr\mu_{ss} + 2h^2 Gr + h^2 G'\mu_{ss} + 7hh'G\mu_{ss}}{6h^3 G^2} \qquad (32c)$$

$$f_1 = \frac{1}{6rh^4 G^2}(-2h^2 h''\text{G'r}^2\mu_{ss} + 2h^2 \text{Gh}^{(3)}r^2\mu_{ss} - 12hh'h''\text{Gr}^2\mu_{ss} + 4hh'^2\text{G'r}^2\mu_{ss} + 12h'^3\text{Gr}^2\mu_{ss} - 2h^3\text{G'r}^2$$

$$+ 2h^2 h''Gr\mu_{ss} - 2h^2 h'r^2 G - 4hh'^2 Gr\mu_{ss} + G'h^3\mu_{ss} + 2h^3 Gr - Gh^2 h'\mu_{ss}) \qquad (32d)$$

$$f_0 = \frac{1}{6r^2 h^4 G^2}(-h^2 h''\text{G'r}^2\mu_{ss} + h^2\text{Gh}^{(3)}r^2\mu_{ss} - 6hh'h''\text{Gr}^2\mu_{ss} + 2hh'^2\text{G'r}^2\mu_{ss} + 6h'^3\text{Gr}^2\mu_{ss} - h^3\text{G'r}^2 \qquad (32e)$$

$$+ h^2 h''Gr\mu_{ss} + G'h'h^2 r\mu_{ss} - h^2 h'r^2 G - 2hh'^2 Gr\mu_{ss} + G'h^3\mu_{ss} + 2h^3 Gr) \qquad (32f)$$

$$f = \frac{1}{6G^2}(2G'\rho''\mu_{ss}\omega^2 r^3 - 2G\rho^{(3)}\mu_{ss}\omega^2 r^3 + 10G'\rho'\mu_{ss}\omega^2 r^2 + 2G\rho'\omega^2 r^3 - 2G'\rho\omega^2 r^3 \qquad (32g)$$

$$-17G\rho''\mu_{ss}\omega^2 r^3 - 33G\rho'\mu_{ss}\omega^2 r + 8G'\rho\mu_{ss}\omega^2 r + 7G\rho\omega^2 r^2 + G'\rho^s\omega^2 r^2 + 6\alpha'\Delta TrG^2 - 12G\rho\mu_{ss}\omega^2 \\ - 4Gr\rho^s\omega^2) \qquad (32h)$$

In Eq. (32) the super index (3) means, the third order differential. Assuming power-law

variation for FGIM material we will have

$$G(r) = G_o \left(\frac{r}{R}\right)^\lambda, \ \rho(r) = \rho_o \left(\frac{r}{R}\right)^m, \ \alpha(r) = \alpha_o \left(\frac{r}{R}\right)^t, \ h(r) = h_o \left(\frac{r}{R}\right)^{-n} \tag{33}$$

where G_0, ρ_0, α_0, h_0 are the shear modulus, the mass density, the thermal expansion coefficient and the disc thickness at a point on the outer surface of the disc. By substituting Eq. (33) into Eqs. (32) and (31), the following equations can be obtained

$$f_4 = -2\mu_{ss}r^4 \tag{34a}$$

$$f_3 = 2\mu_{ss}(\lambda - 3n - 2)r^3 \tag{34b}$$

$$f_2 = (4\lambda n - 6n^2 + \lambda - n)\mu_{ss}r^2 + 2r^4 \tag{34c}$$

$$f_1 = \mu_{ss}(2\lambda n^2 - 2n^3 - 2\lambda n + 4n^2 + \lambda - n)r + (-2\lambda + 2n + 2)r^3 \tag{34d}$$

$$f_0 = -\mu_{ss}(n - 1)^2(\lambda - n) + (\lambda - n - 2)r^2 \tag{34e}$$

$$f = \mu_{ss}h_o R^{n-m}\omega^2\rho_o(m + 2)^2(2\lambda - 2m - 3)r^{3-n+m} + 6th_o R^{n-\lambda-t}G_o\alpha_o\Delta Tr^{3-n+\lambda+t} \tag{34f}$$

$$+h_o R^n\omega^2\rho^s(\lambda - 4)r^{4-n} - h_o R^{n-m}\omega^2\rho_o(2\lambda - 2m - 7)r^{5-n+m} \tag{34g}$$

We use following dimensionless parameters to make Eq. (31) non-dimensional

$$\bar{\varphi} = h_o^{-1}R^{-3}\rho_o^{-1}\omega^{-2}\varphi, \quad \bar{r} = R^{-1}r, \ \bar{\mu}_{ss} = \mu_{ss}R^{-2}, \quad \bar{G}_o = R^{-2}\rho_o^{-1}\omega^{-2}G_o, \ \bar{\rho}^s = R^{-1}\rho_o^{-1}\rho^s \tag{35}$$

then Eq. (31) turns into

$$\bar{f}_4 \frac{\partial^4 \bar{\varphi}}{\partial \bar{r}^4} + \bar{f}_3 \frac{\partial^3 \bar{\varphi}}{\partial \bar{r}^3} + \bar{f}_2 \frac{\partial^2 \bar{\varphi}}{\partial \bar{r}^2} + \bar{f}_1 \frac{\partial \bar{\varphi}}{\partial \bar{r}} + \bar{f}_0 \bar{\varphi} + \bar{f} = 0 \tag{36}$$

where

$$\bar{f}_4 = -2\bar{\mu}_{ss}\bar{r}^4 \tag{37a}$$

$$\bar{f}_3 = 2\bar{\mu}_{ss}(\lambda - 3n - 2)\bar{r}^3 \tag{37b}$$

$$\bar{f}_2 = (4\lambda n - 6n^2 + \lambda - n)\bar{\mu}_{ss}\bar{r}^2 + 2\bar{r}^4 \tag{37c}$$

$$\bar{f}_1 = \bar{\mu}_{ss}(2\lambda n^2 - 2n^3 - 2\lambda n + 4n^2 + \lambda - n)\bar{r} + (-2\lambda + 2n + 2)\bar{r}^3 \tag{37d}$$

$$\bar{f}_0 = -\bar{\mu}_{ss}(n - 1)^2(\lambda - n) + (\lambda - n - 2)\bar{r}^2 \tag{37e}$$

$$\bar{f} = \bar{\mu}_{ss}(m + 2)^2(2\lambda - 2m - 3)\bar{r}^{3-n+m} + 6t\bar{G}_o\alpha_o\Delta T\bar{r}^{3-n+\lambda+t} + \bar{\rho}^s(\lambda - 4)\bar{r}^{4-n}$$
$$- (2\lambda - 2m - 7)\bar{r}^{5-n+m} \tag{37f}$$

For fixed-free condition we can write

$$r = r_0: \begin{cases} u_r = 0 \\ \sigma_r^{nl} (2\pi r_0)h_{in} = \iint \rho r^2\omega^2 h \, dr d\theta \end{cases} \tag{38a, 38b}$$

$$r = R : \begin{cases} \sigma_r^{nl} = 0 \\ \sigma_\theta^{nl} = \sigma \end{cases} \tag{39a, 39b}$$

Assuming we have constant distribution of pressure at the outer radius, σ is an arbitrary constant value.

3.1 DQM solution

To solve Eq. (36) we use differential quadrature method (DQM), which is an efficient numerical method (means with minimum numbers of sample values of a function you will able gain more accurate solution) for the solution of complicated partial and ordinary differential equations and is applicable for all boundary conditions. This method has been inspired from Riemmann summation which is used for calculation definite integral.

$$\int_a^b f(x)\, dx = w_1 f_1 + w_2 f_2 + \cdots + w_n f_n = \sum_{k=1}^n w_k f_k \tag{40}$$

where $w_1, w_2, \ldots, w_n$ are weighting coefficients and $f_1, f_2, \ldots, f_n$ are the functional values at the discrete points $a = x_1, x_2, \ldots, x_n = b$. According to this procedure for "m" order derivative, we can write (Chang 2012)

$$\frac{\partial^m f(x_i)}{\partial x^m} = \sum_{j=1}^N w_{ij}^{(m)} \cdot f(x_j), \text{where } i = 1, 2, \ldots, N, m = 2, 3, \ldots, N-1 \tag{37}$$

In this equation weighting coefficients are calculated from following recurrence relation

$$w_{ij}^{(m)} = m \left[w_{ij}^{(1)} w_{ii}^{(m-1)} - \frac{w_{ij}^{(m-1)}}{x_i - x_j} \right], \qquad w_{ii}^{(m)} = -\sum_{j=1, j \neq i}^N w_{ij}^{(m)} \tag{38}$$

Knowing that

$$w_{ij}^{(1)} = \frac{M^{(1)}(x_i)}{(x_i - x_j) \cdot M^{(1)}(x_j)} \ for\ i \neq j, \qquad w_{ii}^{(1)} = -\sum_{j=1, j \neq i}^N w_{ij}^{(1)}\ ,$$

$$M^{(1)}(x_i) = \prod_{k=1, k \neq i}^N (x_i - x_k) \tag{39}$$

We can use following equation instead of Eq. (38)

$$w_{ij}^{(2)} = \sum_{k=1}^n w_{ik}^{(1)} w_{kj}^{(1)}, w_{ij}^{(3)} = \sum_{k=1}^n w_{ik}^{(1)} w_{kj}^{(2)}, w_{ij}^{(4)} = \sum_{k=1}^n w_{ik}^{(1)} w_{kj}^{(3)}, \ldots, w_{ij}^{(m)}$$

$$= \sum_{k=1}^n w_{ik}^{(1)} w_{kj}^{(m-1)} \tag{40}$$

Remember that distribution of sample points has prominent role in definite convergence. It is better that such distribution be non-uniform and if possible, clustered near boundaries. In the

meanwhile the Chebyshev nodes would be the best choice (Chang 2012)

$$\bar{r}_i = \frac{1 - \bar{r}_0}{2}\left(1 - \cos\left(\frac{i-1}{N-1}\pi\right)\right) + \bar{r}_0 \tag{41}$$

where N is the total number of sample points and $\bar{r}_0 = \bar{r}_{in.}$

4. Numerical results and discussion

Using Poly methyl methacrylate (PMMA) properties as an incompressible material (Schwartz 2008)

$$\rho_o = 1170 \ {kg}/{m^3} \ , E_o = 3 \times 10^9 \ {N}/{m^2} \ , \alpha_o = 9 \times 10^{-10} \ K^{-1} \tag{42}$$

And (Zhen *et al.* 2015)

$$R = r_{ou} = 5 \ \mu m, \qquad h_o = 0.16 \ \mu m, \qquad \omega = 20000 \ rpm, \qquad \Delta T = \frac{\rho_0 \omega^2 R^2}{G_0 \alpha_0} \tag{43}$$

we study the effect of different parameters on stress, strain and displacement of the micro-disc.

4.1 Effect of radius ratio ($c_r = \frac{r_{in}}{r_{ou}}$)
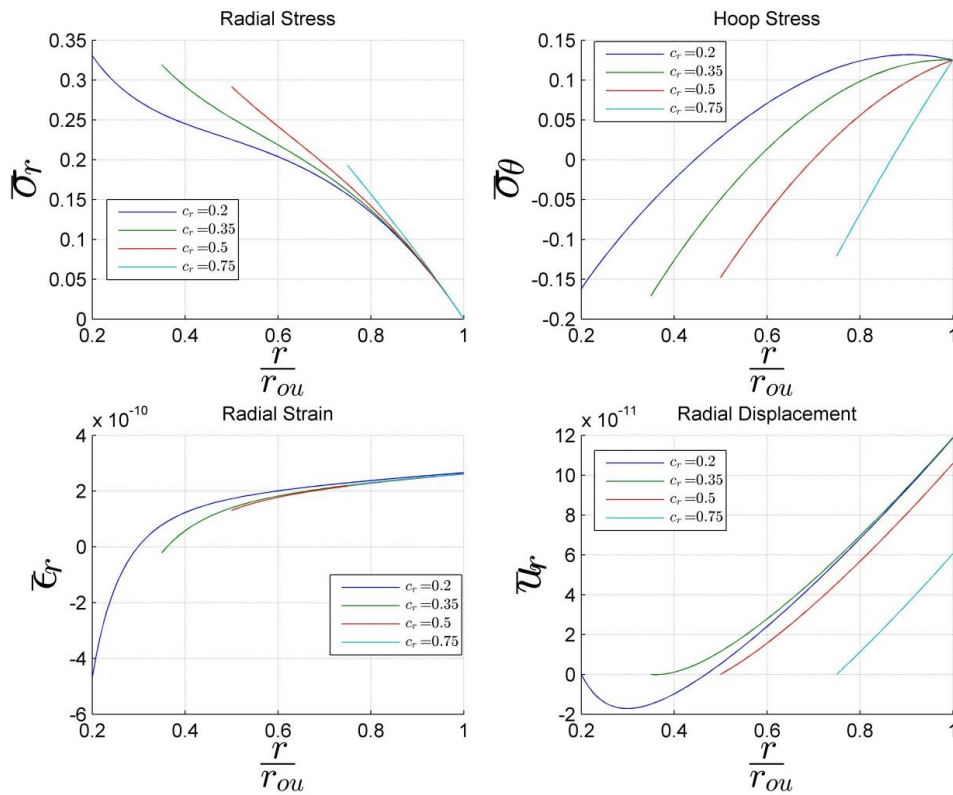

Fig. 3 Effect of inner radius to outer radius while $m = n = \lambda = t = \bar{\rho}^s = \bar{\mu}_{ss} = 1$
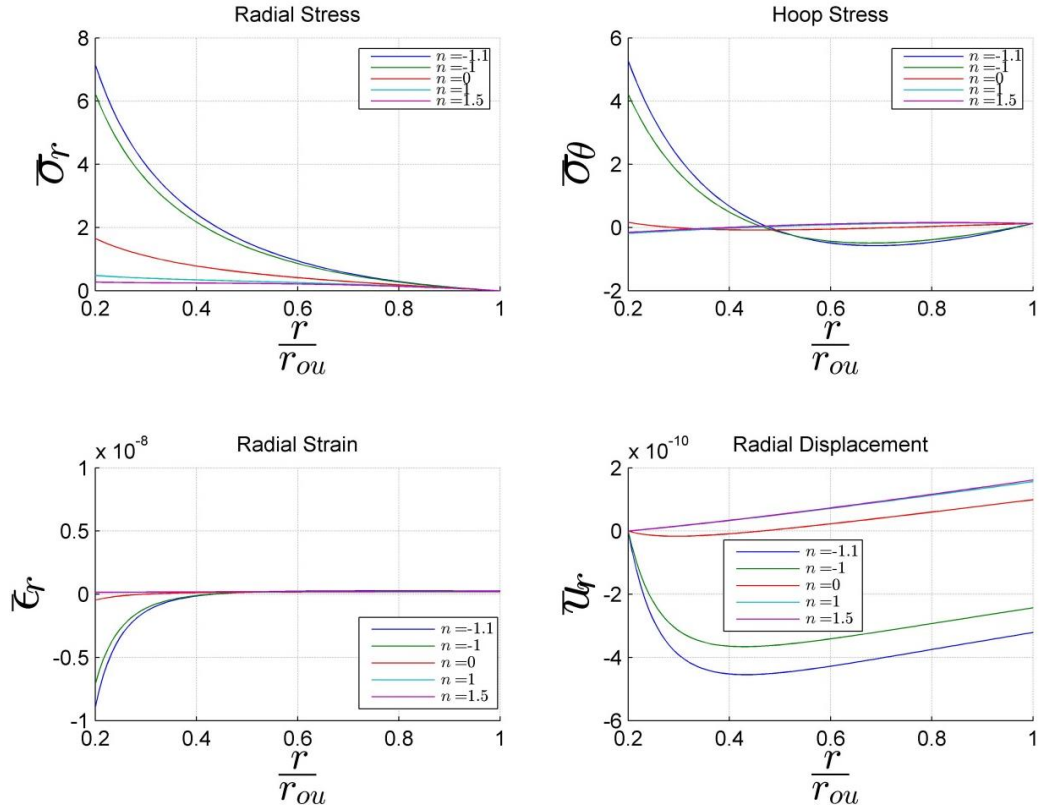
Fig. 4 Effect of thickness while $\mathbf{m} = \mathbf{\lambda} = \mathbf{t} = \mathbf{0}$, $\overline{\mathbf{\rho}}^{\mathbf{s}} = \overline{\mathbf{\mu}}_{\mathbf{ss}} = \mathbf{1}$

Fig. 3 presents, effect of mentioned variation in a situation that thickness, density, shear modulus and thermal expansion follow linear variation pattern.

The first result that is common between all four diagrams is the tendency of linearity when c_r increases. The radial and hoop stresses have completely reverse behavior as c_r increases, so that initial radial stress decreases while corresponding hoop stress with miserly changes starts to rise. They also have inverse behavior when they are coming in to the outer boundary; c_r increasing ends up with steeper reach for radial stress than hoop stress. c_r causes both radial strain and displacement (and thus hoop strain) in a weaker situation when it started to rise. It seems lower strains that take place as a result of c_r increasing, strengthens radial stresses and weakens hoop stresses.

4.2 Effect of thickness(n)

Fig. 4 depicts, influenced behavior by thickness (we have fixed c_r ratio at 0.2). It's assumed that density, shear modulus and thermal expansion are constant.

First, let's see what happens to thickness when "n" increases or decreases; when n is minus, thickness function is increasing, and for positive values of "n" we have decreasing variation for thickness function; this means that for minus values of "n", outer radiuses are thicker and for positive values of "n" inner radius are thicker. On the other hand by increasing "n" at each radius,
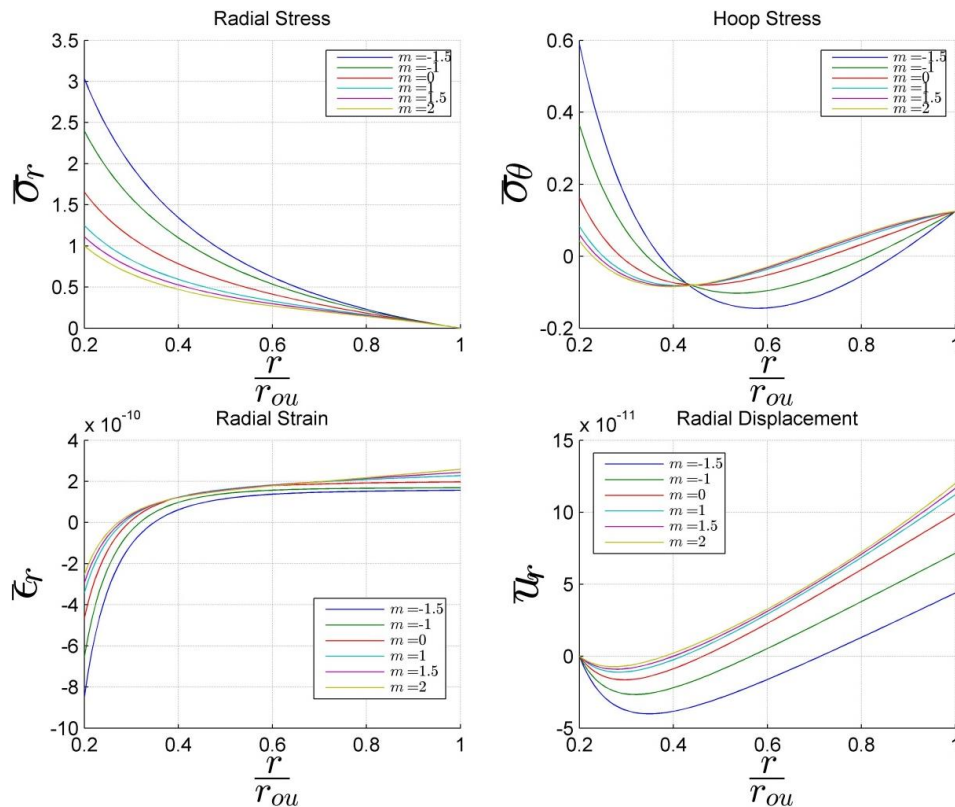
Fig. 5 Effect of density while $\mathbf{n = \lambda = t = 0}, \bar{\boldsymbol{\rho}}^{\mathbf{s}} = \bar{\boldsymbol{\mu}}_{\mathbf{ss}} = \mathbf{1}$

corresponding thickness decreases but the slope of thickness function will be steeper. According to Fig. 4 "n" increasing, has the regular effect on all outputs except on hoop stress. Not to mention hoop stress, by decreasing "n" (meaning increasing thickness at every radius) the absolute value of radial stress, radial strain and displacement boundlessly grows but on the contrary when "n" increases all of the curves converge with each other; it means the thicker micro disc delivers higher tensile radial stress, and higher contractive radial strain and displacement, and thinner disc acts like the thickness linear function (n=1). But in the case of hoop stress, we have two different behaviors, first, when "n" is minus and zero and second, when "n" is positive. In each situation we have an intersect point close to the middle of disc. On the right side of intersect point we have compressive hoop stress and higher thickness delivered higher compressive stress, but anyway we see bounded behavior of hoop stress. The situation is different on the left side of intersect point. With the first case, the hoop stress turns into tensile near the inner radius and again, the thicker disc, the higher tensile hoop stress. But with the second case we have downward concavity, and on the contrary, a thinner disc will have a little more compressive hoop stress. Anyway when the positive "n" increases, hoop stress curves diverge from uniform curve (n=0) and we can say when a micro disc becomes thinner, hoop stress acts like that the thickness is constant. In an overview, radial stresses tend to be tensile and hoop stresses tend to be tensile at inner radius while they are willing to be compressive at outer boundary. The attitudinal behavior of radial strain and displacement is contractive.
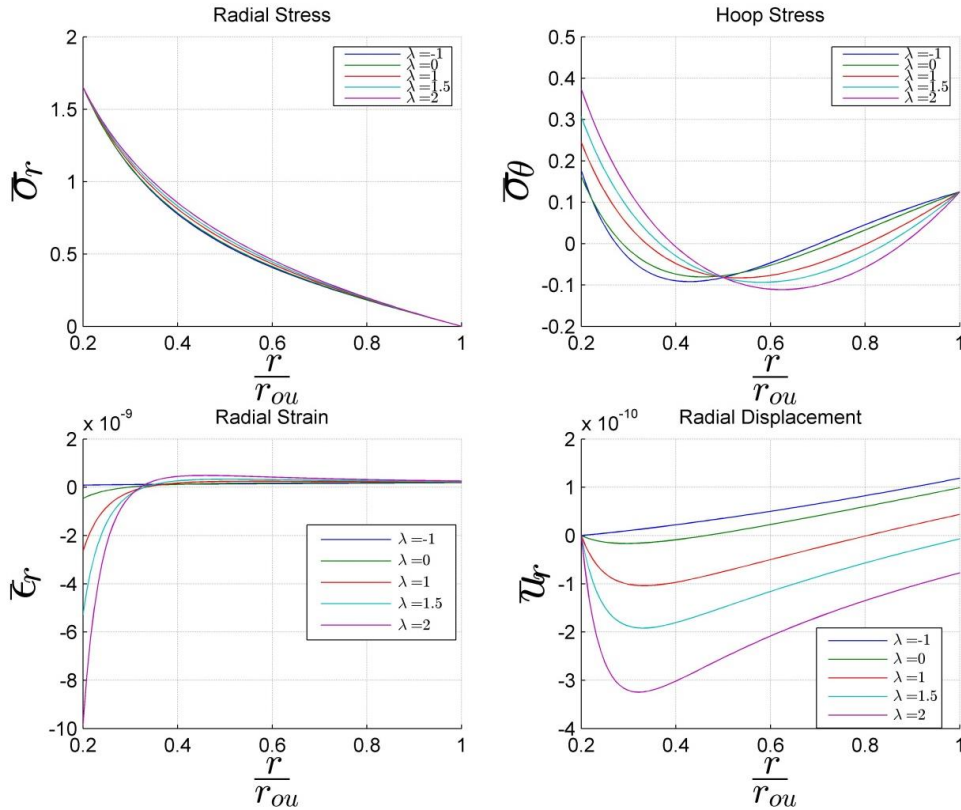
Fig. 6 Effect of shear modulus $\mathbf{m = n = t = 0}$, $\bar{\boldsymbol{\rho}}^{\mathbf{s}} = \bar{\boldsymbol{\mu}}_{\mathbf{ss}} = \mathbf{1}$

4.3 Effect of density(m)

Fig. 5 shows effect of density on outputs while thickness, shear modulus and thermal expansion are constant.

Density of material in each radius is diminished when the power "m" started to rise, instead, falling of "m" dents the material at any radius of disc. As Fig. 5 is showing, a denser micro disc (decreasing "m") diverges radial strain curves and radial displacement curves (and thus hoop strain curves) from each other separately, the more and more, and leads them toward contractive state for displacement, and in result we achieve the stronger tensile radial stress. Again, you can see, when "m" started to increasing, in the other words, when density in each radius becomes thin, the mentioned curves converges with each other and they tend to acts as if density function is linear (m=1).

As thickness effect, there is a conjunction point in hoop stress diagram. When we are in the right side of this point, where we are close to the outer boundary, the stresses tend to be compressive, in return, in the left side of intersecting point they will try to rise in tensile area of diagram.

There is still convergence tendency between the hoop stress curves when density of micro disc in each radius becomes thinner in addition, the thicker density, the higher compressive and tensile hoop stress. In summary, radial stresses tend to be tensile, hoop stresses in the outer tends to be
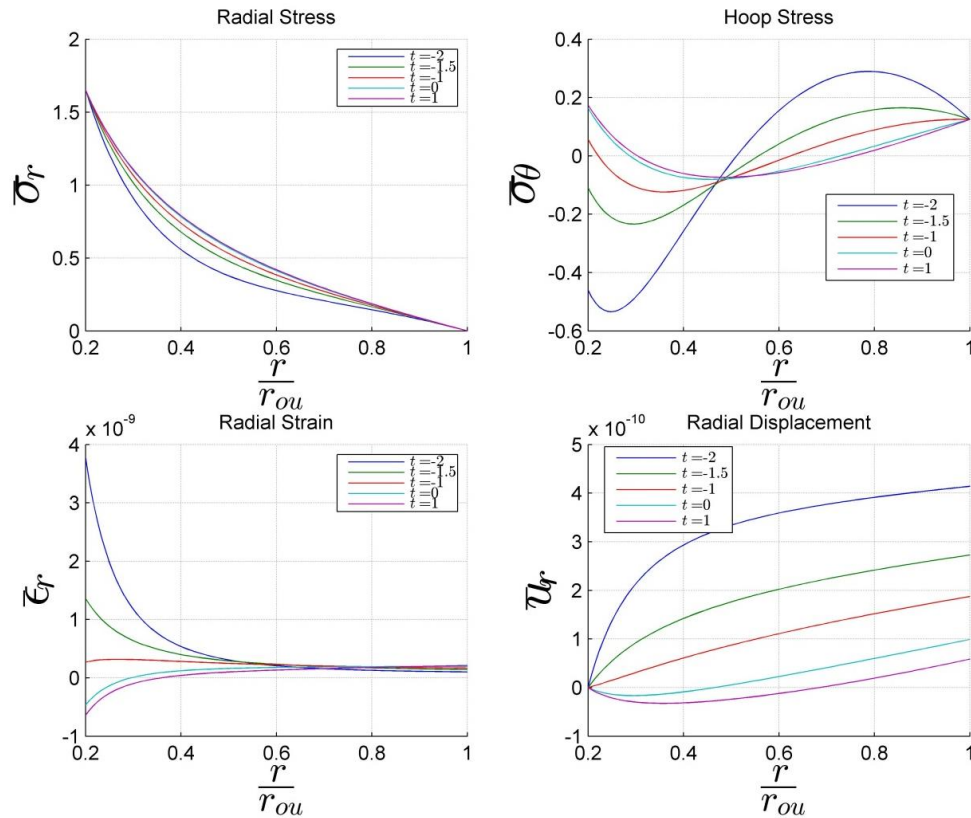
Fig. 7 Effect of thermal expansion while $\mathbf{m} = \boldsymbol{\lambda} = \mathbf{n} = \mathbf{0}$, $\overline{\boldsymbol{\rho}}^{\mathbf{s}} = \overline{\boldsymbol{\mu}}_{\mathbf{ss}} = \mathbf{1}$

compressive while in the inner boundary it becomes vice versa. Radial strain and displacement tends to be compressive.

4.4 Effect of shear modulus (λ)

Fig. 6 is related to effect of shear modulus on outputs, while thickness, density and thermal expansion are constant. This effect on hoop stress, radial strain and radial displacement is the same as effect of density. But in the case of radial stresses, it is visible that related curves tend to convergence with each other. Here, we must not neglect, that the values for radial displacement under influence of changing shear modulus is correspondingly lower than values are influenced by density effect. So we can conclude that radial stresses tend to be tensile which do as a linear variation of shear modulus. Hoop stresses in the outer boundary tend to be compressive while their actions in the inner boundary go toward tensile stresses. The both of radial strain and displacement have contractive tendency.

4.5 Effect of thermal expansion (t)

Assuming shear modulus, density and thermal expansion are constant, Fig. 7 pictures effect of power law variation of thermal expansion on strains, stresses and displacements of micro disc. The
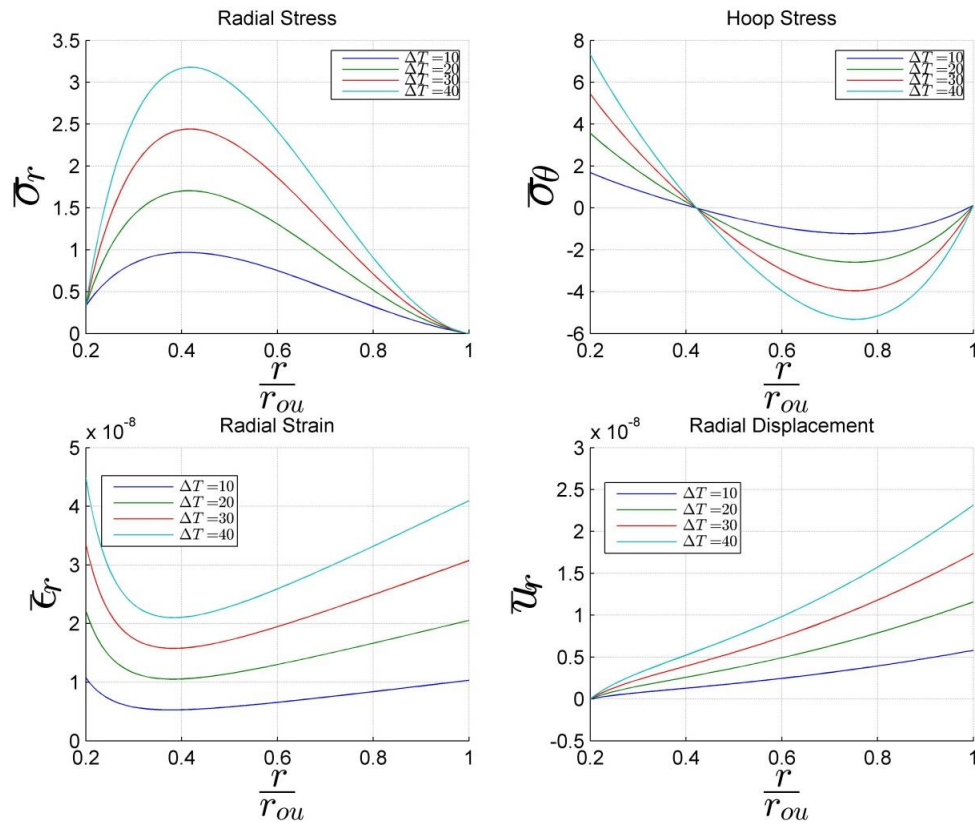
Fig. 8 Effect of uniform temperature rise while $\mathbf{m = \lambda = t = n = \bar{\rho}^s = \bar{\mu}_{ss} = 1}$

rise of "t" rises hoop (near the inner radius) and radial stresses but for radial strain and displacement this effect is vice versa. Also, rising of "t" converges all of curves with each other, however, in this case the radial stress curves are innately convergent. Intersecting point that discussed in above clauses exists here, too. Hoop stress in the outer boundary tends to be compressive but in the inner boundary their tendency is tensile state. Like before, radial stresses have tensile attitudinal behavior. Unlike previous cases, here, radial strains and displacements tend to be expansionary.

4.6 Effect of temperature rise (ΔT)

Supposing all radial variations are linear, Fig. 8 depicts effect of uniform temperature rise on the discussed outputs. When the temperature rise becomes very little (in the tenth and hundredth or lower) the curves completely converge with each other, for this reason we has used higher values for ΔT to make visible behavior of all out puts.

As you can see in Fig. 8 except for radial stress all manners are like thermal expansion variation. With a glance at Fig. 8 we are able to find that ΔT is trying to put micro disc in the compressive hoop stresses state while thermal expansion (previous discussion) resists to this action. Increasing of ΔT diverges radial stresses from each other. There is no limited behavior in this case, unless ΔT is very little. For the case of micro devices such as gas turbines (MGTs) we
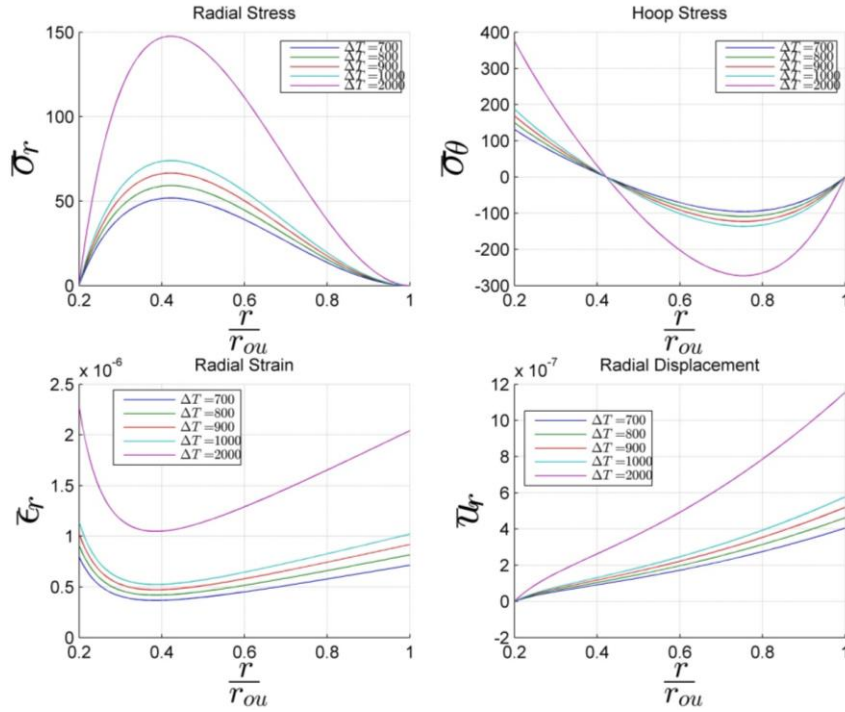
Fig. 9 Effect of uniform temperature rise for micro gas turbine situation while $\mathbf{m = \lambda = t = n = \overline{\rho}^s = \overline{\mu}_{ss} = 1}$
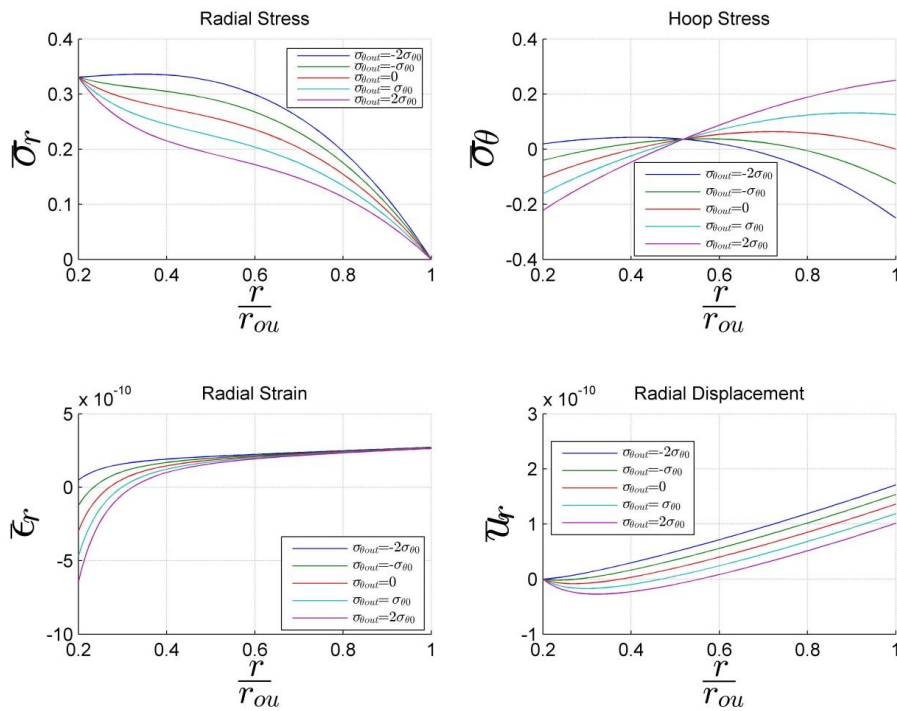
Fig. 10 Effect of outer boundary condition while $\mathbf{m = \lambda = t = n = \overline{\rho}^s = \overline{\mu}_{ss} = 1}$
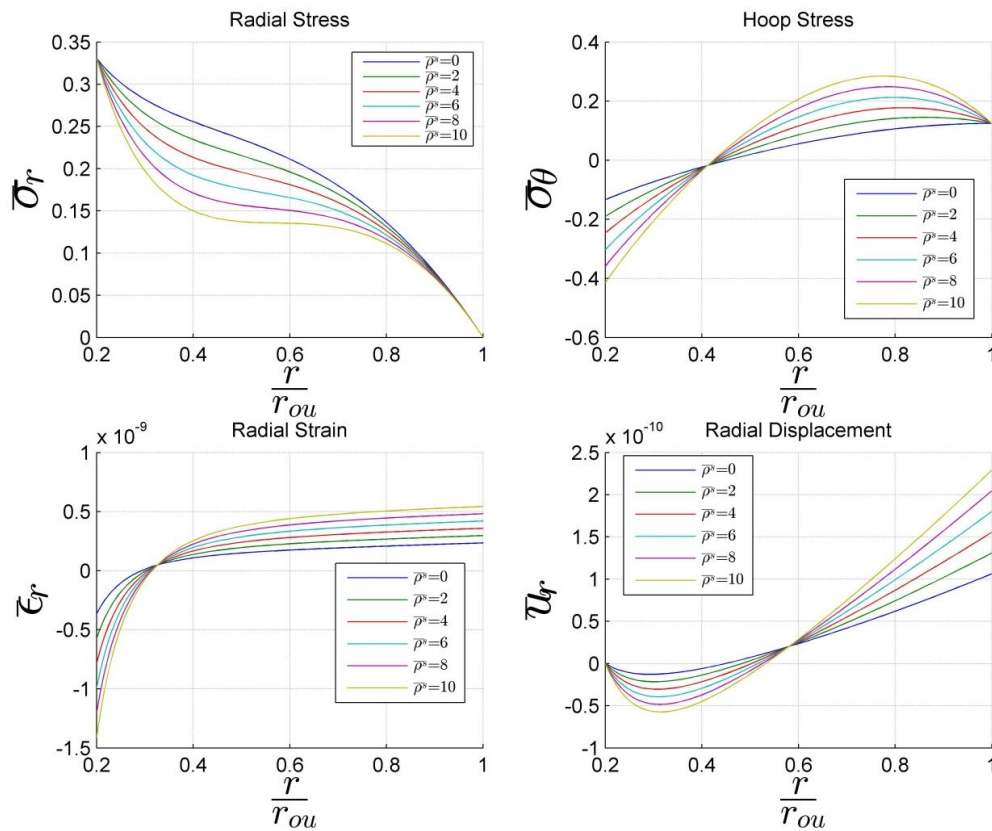
Fig. 11 Effect of surface condition while $m = \lambda = t = n = \bar{\mu}_{ss} = 1$

have drawn another exaggerated diagram (Fig. 9). For the MGTs the inside temperature for MGTs reaches up to 950°C; we have consider temperature rise of 2000°C (K) too much larger than glass transition temperature only to show what happened if the glass transition temperature (the temperature between solid and liquid state transition) would be large up to 2000°C. As you can see for a FGIM that the outer surface made of PMMA, like PVC/PMMA the maximum non dimensional tensile stress would be about 400; in worse situation the tensile stress of PVC/PMMA combination is 4.5 kgf/mm2 (Schwartz 2008) , or 3.5e+8 non dimension value that is too big than 400.

As you know one of the features of incompressible material is their good resistance in front of compression. Also you can see that radial displacement in crises situation would be 1.2e-4 that is noticeable for fit-up goals. However, considering that glass transition temperature is too much less 2000°C, we can conclude for temperature that is under glass transition temperature, FGIMs can be one of appropriate choices.

4.7 Effect of outer boundary condition

Fig. 10 is related to different outer boundary conditions. Increasing the value of outer boundary condition alters the slope of radial stresses and weakens them miserly. Outer hoop stress falling
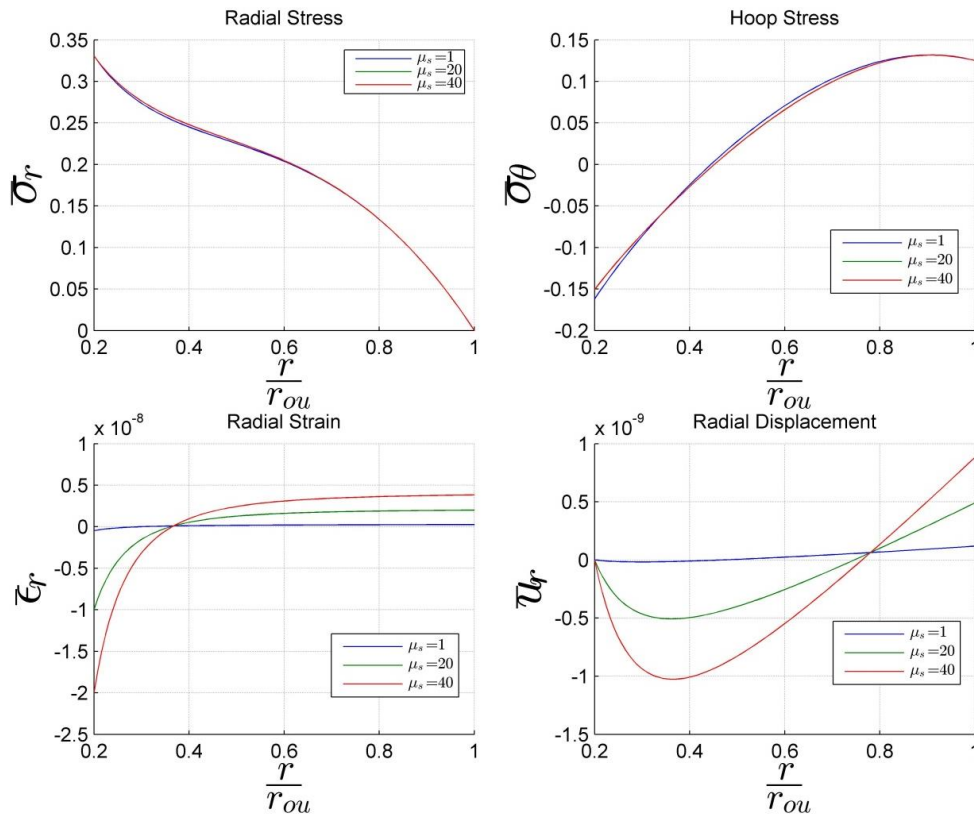
Fig. 12 Effect of nonlocal parameter while $m = \lambda = t = n = \bar{\rho}^s = 1$

cannot rises inner hoop stress continuously and after some steps rising speed of hoop stress at the inner radius is lowered. Radial strain reaches in limited state by decreasing the value of outer hoop stress boundary condition; Radial displacement curves, have similar states in each value of boundary condition which results in parallel curves as you can see in Fig. 10.

4.8 Effect of surface ($\bar{\rho}^s$)

Fig. 11 depicts effect of surface on introduced outputs. The first thing that is visible in all diagrams is convergence feature of them. We have seen the effect of this feature on previous studied cases. Radial stresses tend to be tensile. Existence of intersect point in hoop stress, radial strain and radial displacement causes contradictory behaviors on both sides of disc; the hoop stresses on the right side of intersect point tend to be tensile while they tends to be compressive at the left side of mentioned point. The behavior of radial strain and displacement is the same as hoop stress, except that tensile state covers most part of the disc for hoop stress and radial strain.

4.9 Effect of nonlocal parameter ($\bar{\mu}_{ss}$)

Fig. 12 pictures, the effect of nonlocal parameter on intended outputs. There is strictly convergence in plotted diagrams so we forced to use large interval between our steps. It seems the
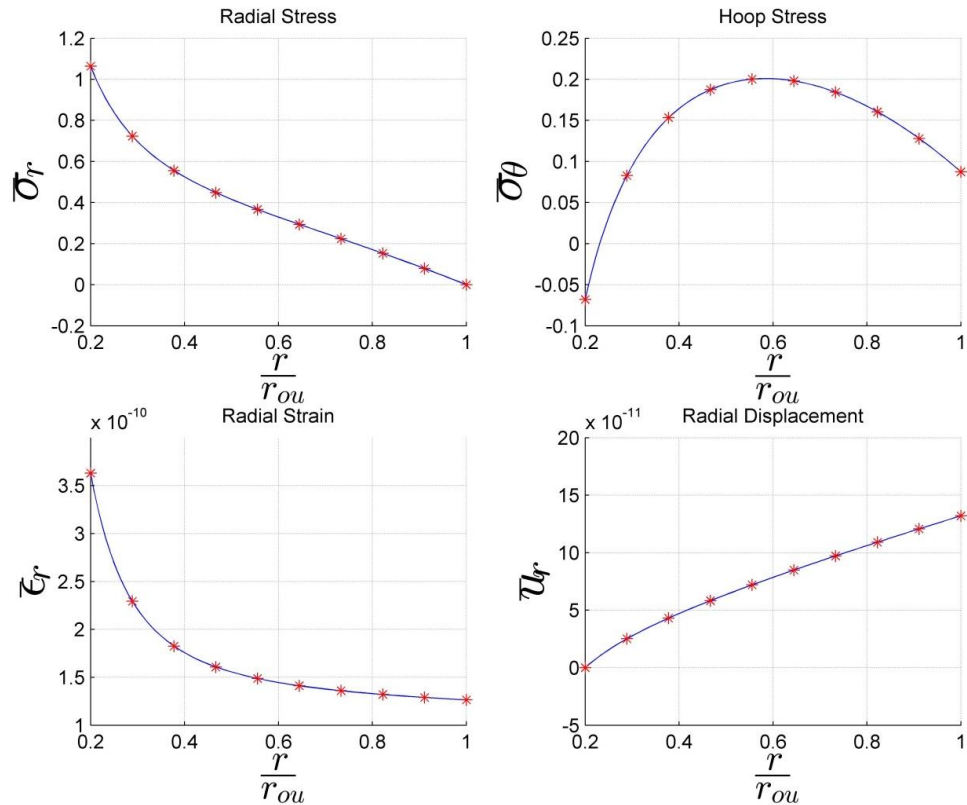
Fig. 13 Verification diagram $m = t = n = \bar{\rho}^s = \bar{\mu}_{ss} = 0$, $\lambda = 1$, the (*) related to Reference (Nie and Batra 2010) and continuous line related to present research

convergent effect of nonlocal parameter on previous studied cases be more than the same effect of surface stress. Under effect of nonlocal parameter radial stresses tend to be in tensile state. Propagation of hoop stresses in the area of tensile and compressive stresses is similar and we don't see any excellence in these fields. However, about radial strain and displacement it's visible that in the outer radiuses, expansionary state is dominant while in the large part of disc around the inner radius, contractive state has prominent role in behavior of radial displacement.

5. Conclusions

We studied effect of different input specially nonlocal and surface on stresses and strains in a rotating micro disc on the uniform thermal loading. We saw that the surface tends to split situation over the micro disc to compressive and tensile, while nonlocal parameters tries by converging, assimilate deferent behaviors. The nonlocal parameter tendency to converge the studied curves, is decreased by increasing temperature rise; needless to say that we don't see sudden changes in hoop and radial stresses (Fig. 8 and Fig. **9**). We also concluded under glass transition temperature FGIMs are able to act very well. To verify our result it is enough to set the value of nonlocal and

surface parameters to zero and compare gained values with similar articles; as you can see in figure Fig. 13, the nonlocal and surface solution (continuous line) is coincides with previous analytical study (Nie and Batra 2010).

References

Agari, Y., Anan, Y., Nomura, R. and Kawasaki, Y. (2007), "Estimation of the compositional gradient in a PVC/PMMA graded blend prepared by the dissolution-diffusion method", *Polym.*, **48**(4), 1139-1147.

Agari, Y., Shimada, M., Ueda, A. and Nagai, S. (1996), "Preparation, characterization and properties of gradient polymer blends: discussion of poly (vinyl chloride)/poly (methyl methacrylate) blend films containing a wide compositional gradient phase", *Macromol. Chem. Phys.*, **197**(6), 2017-2033.

Agari, Y. (2002), "Polymer blends, functionally graded", *Encyclopedia Smart Mater.*, John Wiley and Sons, U.S.A.

Aichmayer, L., Spelling, J., Laumert, B. and Fransson, T. (2013), "Micro gas-turbine design for small-scale hybrid solar power plants", *J. Eng. Gas Turb. Power*, **135**(11), 113001.

Anani, Y. and Rahimi, G.H. (2016), "Stress analysis of rotating cylindrical shell composed of functionally graded incompressible hyperelastic materials", *Int. J. Mech. Sci.*, **108**, 122-128.

Bilgili, E. (2003), "Controlling the stress-strain inhomogeneities in axially sheared and radially heated hollow rubber tubes via functional grading", *Mech. Res. Comm.*, **30**(3), 257-266.

Bilgili, E. (2004), "Functional grading of rubber tubes within the context of a molecularly inspired finite thermoelastic model", *Acta Mech.*, **169**(1-4), 79-85.

Carmine L. and Quadrini, F. (2009), "Indentation of functionally graded polyester composites", *Measurement*, **42**(6), 894-902.

Çetin, E., Kurşun, A., Aksoy, Ş. and Çetin, M.T. (2014), "Elastic stress analysis of annular bi-material discs with variable thickness under mechanical and thermomechanical loads", World Academy of Science, Engineering and Technology, *Int. J. Mech.*, *Aerospace*, *Ind.*, *Mechatronic Manuf. Eng.*, **8**(2), 288-292.

Chakraborty, A., Dutta, A.K., Ray, K.K. and Subrahmanyam, J. (2009), "An effort to fabricate and characterize in-situ formed graded structure in a ceramic-metal system", *J. Mater. Process. Technol.*, **209**(5), 2681-2692.

Ding, S., Li, Y. and Li, G. (2014), "Evaluation of thermal loadings to ameliorate stress in a rotating disk", *J. Thermophys. Heat Transf.*, **28**(4), 667-678.

Dryden, J.R. and Batra, R.C. (2013), "Material tailoring and moduli homogenization for finite twisting deformations of functionally graded Mooney-Rivlin hollow cylinders", *Acta Mech.*, **224**(4), 811-818.

Ebrahimi F. and Rastgoo, A. (2008a), "Free vibration analysis of smart annular FGM plates integrated with piezoelectric layers", *Smart Mater. Struct.*, **17**(1), 015044.

Ebrahimi F. and Rastgoo, A. (2008b), "An analytical study on the free vibration of smart circular thin FGM plate based on classical plate theory", *Thin Wall. Struct.*, **46**(12), 1402-1408.

Ebrahimi F. and Rastgoo, A. (2008c), "Free vibration analysis of smart FGM plates", *Int. J. Mech. Sys. Sci. Eng.*, **2**(2), 94-99.

Ebrahimi F. and Daman, M. (2016), "Dynamic modeling of embedded curved nanobeams incorporating surface effects", *Coupled Syst. Mech.*, **5**(3), 255-268.

Ebrahimi F., Rastgoo, A. and Atai, A.A. (2009a), "Theoretical analysis of smart moderately thick shear deformable annular functionally graded plate", *Eur. J. Mech. A-Solid.*, **28**(5), 962-997.

Ebrahimi, F. (2013), "Analytical investigation on vibrations and dynamic response of functionally graded plate integrated with piezoelectric layers in thermal environment", *Mech. Adv. Mater. Struct.*, **20**(10), 854-870.

Ebrahimi, F. and Salari, E. (2015a), "Size-dependent thermo-electrical buckling analysis of functionally graded piezoelectric nanobeams", *Smart Mater. Struct.*, **24**(12), 125007.

Ebrahimi, F. and Salari, E. (2015b), "Nonlocal thermo-mechanical vibration analysis of functionally graded

nanobeams in thermal environment", *Acta Astronaut.*, **113**, 29-50.

Ebrahimi, F. and Salari, E. (2015c) "Size-dependent free flexural vibrational behavior of functionally graded nanobeams using semi-analytical differential transform method", *Compos. Part B-Eng.*, **79**, 156-169.

Ebrahimi, F. and Salari, E. (2015d), "A semi-analytical method for vibrational and buckling analysis of functionally graded nanobeams considering the physical neutral axis position", *CMES: Comput. Model. Eng. Sci.*, **105**(2), 151-181.

Ebrahimi, F. and Salari, E. (2015e), "Thermal buckling and free vibration analysis of size dependent Timoshenko FG nanobeams in thermal environments", *Compos. Struct.* **128**, 363-380.

Ebrahimi, F. and Salari, E. (2015f), "Thermo-mechanical vibration analysis of nonlocal temperature-dependent FG nanobeams with various boundary conditions", *Compos. Part B-Eng.*, **78**, 272-290.

Ebrahimi, F. and Barati, M.R. (2016a), "Magneto-electro-elastic buckling analysis of nonlocal curved nanobeams", *Euro. Phys. J. Plus*, **131**(9), 346.

Ebrahimi, F. and Barati, M.R. (2016b), "Static stability analysis of smart magneto-electro-elastic heterogeneous nanoplates embedded in an elastic medium based on a four-variable refined plate theory", *Smart Mater. Struct.*, **25**(10), 105014.

Ebrahimi, F. and Barati, M.R. (2016c), "Temperature distribution effects on buckling behavior of smart heterogeneous nanosize plates based on nonlocal four-variable refined plate theory", *Int. J. Smart Nano Mater.*, **7**(3), 1-25.

Ebrahimi, F. and Barati, M.R. (2016d), "An exact solution for buckling analysis of embedded piezoelectro-magnetically actuated nanoscale beams", *Adv. Nano Res*, **4**(2), 65-84.

Ebrahimi, F. and Barati, M.R. (2016e), "Buckling analysis of smart size-dependent higher order magneto-electro-thermo-elastic functionally graded nanosize beams", *J. Mech.*, **33**(1), 1-11.

Ebrahimi, F. and Barati, M.R. (2016f), "A nonlocal higher-order shear deformation beam theory for vibration analysis of size-dependent functionally graded nanobeams", *Arab. J Sci. Eng.*, **41**(5), 1679-1690.

Ebrahimi, F. and Barati, M.R. (2016g), "Vibration analysis of smart piezoelectrically actuated nanobeams subjected to magneto-electrical field in thermal environment", *J. Vib. Control*, **24**(3), 549-564.

Ebrahimi, F. and Barati, M.R. (2016h), "Buckling analysis of nonlocal third-order shear deformable functionally graded piezoelectric nanobeams embedded in elastic medium", *J. Brazil. Society Mech. Sci. Eng.*, **39**(3), 1-16.

Ebrahimi, F. and Barati, M.R. (2016i), "Small scale effects on hygro-thermo-mechanical vibration of temperature dependent nonhomogeneous nanoscale beams", *Mech. Adv. Mater. Struct.*, Submitted.

Ebrahimi, F. and Barati, M.R. (2016j), "Dynamic modeling of a thermo-piezo-electrically actuated nanosize beam subjected to a magnetic field", *Appl. Phys. A*, **122**(4), 1-18.

Ebrahimi, F. and Barati, M.R. (2016k), "Magnetic field effects on buckling behavior of smart size-dependent graded nanoscale beams", *Eur. Phys. J. Plus*, **131**(7), 1-14.

Ebrahimi, F. and Barati, M.R. (2016l), "Vibration analysis of nonlocal beams made of functionally graded material in thermal environment", *Eur. Phys. J. Plus*, **131**(8), 279.

Ebrahimi, F. and Barati, M.R. (2016m), "A nonlocal higher-order refined magneto-electro-viscoelastic beam model for dynamic analysis of smart nanostructures", *Int. J. Eng. Sci.*, **107**, 183-196.

Ebrahimi, F. and Barati, M.R. (2016n), "Small-scale effects on hygro-thermo-mechanical vibration of temperature-dependent nonhomogeneous nanoscale beams", *Mech. Adv. Mater. Struct.*, **24**(11), 1-13.

Ebrahimi, F. and Barati, M.R. (2016o), "A unified formulation for dynamic analysis of nonlocal heterogeneous nanobeams in hygro-thermal environment", *Appl. Phys. A*, **122**(9), 792.

Ebrahimi, F. and Barati, M.R. (2016p), "Electromechanical buckling behavior of smart piezoelectrically actuated higher-order size-dependent graded nanoscale beams in thermal environment", *Int. J. Smart Nano Mater.*, **7**(2), 69-90.

Ebrahimi, F. and Barati, M.R. (2016q), "Wave propagation analysis of quasi-3D FG nanobeams in thermal environment based on nonlocal strain gradient theory", *Appl. Phys. A*, **122**(9), 843.

Ebrahimi, F. and Barati, M.R. (2016r), "Flexural wave propagation analysis of embedded S-FGM nanobeams under longitudinal magnetic field based on nonlocal strain gradient theory", *Arab. J. Sci. Eng.*,

1-12.

Ebrahimi, F. and Barati, M.R. (2016s), "On nonlocal characteristics of curved inhomogeneous Euler-Bernoulli nanobeams under different temperature distributions", *Appl. Phys. A*, **122**(10), 880.

Ebrahimi, F. and Barati, M.R. (2016t), "Buckling analysis of piezoelectrically actuated smart nanoscale plates subjected to magnetic field", *J. Intell. Mater. Syst. Struct.*, **28**(11), 1472-1490.

Ebrahimi, F. and Barati, M.R. (2016u), "Size-dependent thermal stability analysis of graded piezomagnetic nanoplates on elastic medium subjected to various thermal environments", *Appl. Phys. A*, **122**(10), 910.

Ebrahimi, F. and Barati, M.R. (2016v), "Magnetic field effects on dynamic behavior of inhomogeneous thermo-piezo-electrically actuated nanoplates", *J. Brazil. Society Mech. Sci. Eng.*, **39**(6), 1-21.

Ebrahimi, F. and Barati, M.R. (2017a), "Hygrothermal effects on vibration characteristics of viscoelastic FG nanobeams based on nonlocal strain gradient theory", *Compos. Struct.*, **159**, 433-444.

Ebrahimi, F. and Barati, M.R. (2017b), "A nonlocal strain gradient refined beam model for buckling analysis of size-dependent shear-deformable curved FG nanobeams", *Compos. Struct.*, **159**, 174-182.

Ebrahimi, F. and Hosseini, S.H.S. (2016a), "Double nanoplate-based NEMS under hydrostatic and electrostatic actuations", *Eur. Phys. J. Plus*, **131**(5), 1-19.

Ebrahimi, F. and Hosseini, S.H.S. (2016b), "Nonlinear electroelastic vibration analysis of NEMS consisting of double-viscoelastic nanoplates", *Appl. Phys. A*, **122**(10), 922.

Ebrahimi, F. and Hosseini, S.H.S. (2016c), "Thermal effects on nonlinear vibration behavior of viscoelastic nanosize plates", *J. Therm. Stress.*, **39**(5), 606-625.

Ebrahimi, F. and Mokhtari, M. (2015), "Transverse vibration analysis of rotating porous beam with functionally graded microstructure using the differential transform method", *J. Brazil. Society Mech. Sci. Eng.*, **37**(4), 1435-1444.

Ebrahimi, F. and Nasirzadeh, P. (2015), "A nonlocal Timoshenko beam theory for vibration analysis of thick nanobeams using differential transform method", *J. Theor. Appl. Mech.*, **53**(4), 1041-1052.

Ebrahimi, F. and Salari, E. (2016), "Effect of various thermal loadings on buckling and vibrational characteristics of nonlocal temperature-dependent functionally graded nanobeams", *Mech. Adv. Mater. Struct.*, **23**(12), 1379-1397.

Ebrahimi, F. and Zia, M. (2015), "Large amplitude nonlinear vibration analysis of functionally graded Timoshenko beams with porosities", *Acta Astronaut.*, **116**, 117-125.

Ebrahimi, F., Barati, M.R. and Haghi, P. (2017), "Thermal effects on wave propagation characteristics of rotating strain gradient temperature-dependent functionally graded nanoscale beams", *J. Therm. Stress.*, **40**(5), 535-547.

Ebrahimi, F., Ghadiri, M., Salari, E., Hoseini, S.A.H. and Shaghaghi, G.R. (2015b), "Application of the differential transformation method for nonlocal vibration analysis of functionally graded nanobeams", *J. Mech. Sci. Tech.*, **29**(3), 1207-1215.

Ebrahimi, F., Ghasemi, F. and Salari, E. (2016a), "Investigating thermal effects on vibration behavior of temperature-dependent compositionally graded Euler beams with porosities", *Meccan.*, **51**(1), 223-249.

Ebrahimi, F., Naei, M.H. and Rastgoo, A. (2009b), "Geometrically nonlinear vibration analysis of piezoelectrically actuated FGM plate with an initial large deformation", *J. Mech. Sci. Technol.*, **23**(8), 2107-2124.

Ebrahimi, F., Rastgoo, A. and Kargarnovin, M.H. (2008), "Analytical investigation on axisymmetric free vibrations of moderately thick circular functionally graded plate integrated with piezoelectric layers", *J. Mech. Sci. Technol.*, **22**(6), 1058-1072.

Ebrahimi, F., Salari, E. and Hosseini, S.A.H. (2015), "Thermomechanical vibration behavior of FG nanobeams subjected to linear and non-linear temperature distributions", *J. Therm. Stress.*, **38**(12), 1360-1386.

Ebrahimi, F., Salari, E. and Hosseini, S.A.H. (2016c), "In-plane thermal loading effects on vibrational characteristics of functionally graded nanobeams", *Meccan.*, **51**(4), 951-977.

Ebrahimi, F., Gholam, R.S. and Boreiry, M. (2016), "An investigation into the influence of thermal loading and surface effects on mechanical characteristics of nanotubes", *Struct. Eng. Mech.*, **57**(1), 179-200.

Eraslan, A.N. and Akis, T. (2015), "On the plane strain and plane stress solutions of functionally graded

rotating solid shaft and solid disk problems", *Acta Mech.*, **181**(1-2), 43-63.

Eraslan, A.N. and Arslan, E. (2015), "Analytical and numerical solutions to a rotating FGM disk", *J. Multidiscip. Eng. Sci. Technol.*, **2**(10), 2843-2850.

Eringen, A.C. (2002), *Nonlocal Continuum Field Theories*, Springer Science and Business Media, U.S.A.

Gurtin, M.E. and Murdoch, A.I. (1975), "A continuum theory of elastic material surfaces", *Arch. Ration. Mech. An.*, **57**(4), 291-323.

Horgan, C.O. and Chan, A.M. (1999), "The stress response of functionally graded isotropic linearly elastic rotating disks", *J. Elasticity*, **55**(3), 219-230.

Hosseini, M. and Dini, A. (2015), "Magneto-thermo-elastic response of a rotating functionally graded cylinder", *Struct. Eng. Mech.*, **56**(1), 137-156.

Jahed, H., Farshi, B. and Bidabadi, J. (2005), "Minimum weight design of inhomogeneous rotating discs", *Int. J. Pressure Vessels Piping*, **82**(1), 35-41.

Kordkheili, S.A.H. and Naghdabadi, R. (2007), "Thermoelastic analysis of a functionally graded rotating disk", *Compos. Struct.*, **79**(4), 508-516.

Leu, S.Y. and Chien, L.C. (2015), "Thermoelastic analysis of functionally graded rotating disks with variable thickness involving non-uniform heat source", *J. Therm. Stress.*, **38**(4), 415-426.

Lu, Pin, He, L.H., Lee, H.P. and Lu, C. (2006), "Thin plate theory including surface effects", *Int. J. Solid. Struct.*, **43**(16), 4631-4647.

Mott, P.H., Dorgan, J.R. and Roland, C.M. (2008), "The bulk modulus and poisson's ratio of "incompressible" materials", *J. Sound Vib.*, **312**(4), 572-575.

Nie, G.J. and Batra, R.C. (2010), "Stress analysis and material tailoring in isotropic linear thermoelastic incompressible functionally graded rotating disks of variable thickness", *Compos. Struct.*, **92**(3), 720-729.

Rajagopal, K.R. (2008), "Boundary layers in finite thermoelasticity", *J. Elasticity*, **36**(3), 271-301.

Schwartz, M. (2008), *Smart Materials*, CRC Press, U.S.A.

Shu, C. (2012), *Differential Quadrature and Its Application in Engineering*. Springer Science and Business Media, U.S.A.

Timoshenko, S.P. and Goodier, J.N. (1970), *Theory of Elasticity*, 3rd ed., McGraw-Hill, U.S.A.

Tutuncu, N. and Temel, B. (2013), "An efficient unified method for thermoelastic analysis of functionally graded rotating disks of variable thickness", *Mech. Adv. Mater. Struct.*, **20**(1), 38-46.

Zafarmand, H. and Kadkhodayan, M. (2015), "Nonlinear analysis of functionally graded nanocomposite rotating thick disks with variable thickness reinforced with carbon nanotubes", *Aerosp. Sci. Technol.*, **41**, 47-54.

Zamani, S.A., Omran, S.T., Asadi, B., and Hosseinzadeh, M. (2014), "Numerical simulation and plan stress analytical solution of rotating disk in high speed", *Indian J. Sci. Res.* **3**(1), 124-136.

Zenkour, A.M. (2006), "Thermoelastic solutions for annular disks with arbitrary variable thickness", *Struct. Eng. Mech.*, **24**(5), 515-528.

Zhen, L., Yong-kai, Q. and Lai-he, Z. (2015), "Heat transfer measurements on a micro disk with high rotational speed", *Proceedings of International Conference on Structural, Mechanical and Materials Engineering*, Dalian, China, November.

Zhou, D., Mei, J., Chen, J., Zhang, H., and Weng, S. (2014), "Parametric analysis on hybrid system of solid oxide fuel cell and micro gas turbine with CO_2 capture", *J. Fuel Cell Sci. Technol.* **11**(5) 051001.

Zhu, X. and Li, L. (2017), "Twisting statics of functionally graded nanotubes using Eringen's nonlocal integral model", *Compos. Struct.*, **178**, 87-96.

EC